Surface Spectroscopy of Room-temperature Ionic Liquids on a Platinum Electrode: A Sum Frequency Generation Study

Selimar Rivera-Rubero and Steven Baldelli*

Department of Chemistry, University of Houston, Houston, Texas 77204

Received: April 21, 2004; In Final Form: June 1, 2004

Sum frequency generation vibrational spectroscopy (SFG) and cyclic voltammetry (CV) measurements have been conducted on the ionic liquid/platinum electrode system. The room-temperature ionic liquid investigated is 1-butyl-3-methylimidazolium $[BMIM]^+$ with $[PF_6]^-$ or $[BF_4]^-$ anions. SFG spectra are taken in situ under potential control from 2750 to 3300 cm^{-1} (C−H stretching region). Polarization-dependent SFG spectra are used to extract orientation information for the cation at the electrode surface. The SFG spectra indicate that the cation changes orientation as the electrode potential is changed within the double-layer region. The plane of the imidazolium ring tips from 35° at positive surface charge to ∼60° from the surface normal at negative surface charge. Further, the orientation change is different for $[BMIM][PF_6]$ than for $[BMIM][BF_4]$. A model for ions at the surface is presented based on these spectroscopic and electrochemical measurements.

Introduction

Room-temperature ionic liquids are liquids composed only of ions and are similar to molten salts such as NaCl.[1] However, a weak interaction between the ions allows them to be liquid at room temperature.[1] Due to the high ionic conductivity, nonvolatility, low vapor pressure, thermal stability, hydrophobicity, and wide electrochemical window that ionic liquids possess, these compounds have become a novel solution to problems encountered with organic solvents and these molecules are a prospective solution to the limitations encountered in electrochemical systems.[2,3] These physical properties can be varied by selecting different combinations of ions.[4−6] Since the electrochemical window of the pure ionic liquids depends on the electrochemical stability of the cation and/or anion, understanding the ion behavior at the electrode surface leads to improvement and implementation of the ionic liquid to the desired system.[7]

Ionic liquids have been used in different systems such as electrochemical cells,[2,3,8,9] fuel cells,[10,11] solar cells,[12,13] liquid−liquid extraction systems,[14,15] and biphasic catalysis processes.[16,17] These systems depend on the interactions at the interface for their performance; unfortunately, the interfacial properties are not well characterized. To enhance the properties of the ionic liquids and expand their applications, it is necessary to understand their behavior at the interface. The electrochemical behavior of haloaluminate ionic liquids has been widely studied, but since their applications are limited due to their moisture sensitivity the attention has been recently focused on more-stable ionic liquids such as those containing imidazolium-based cations (Figure 1) and anions such as hexafluorophosphate, tetrafluoroborate, and others.[7,18−20]

This paper reports the results from sum frequency generation vibrational spectroscopy of $[BMIM][BF_4]$ and $[BMIM][PF_6]$ on a platinum electrode under potential control. These experiments suggest that the imidazolium ring (Figure 1) reorients at the surface in response to the surface charge with the ring orienting more parallel to the surface at negative surface charge.

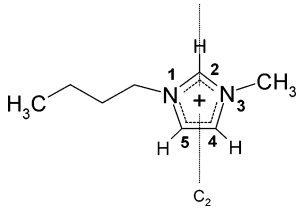

Figure 1. Structure of 1-butyl-3-methylimidazolium cation, $[BMIM]^+$, with numbering scheme and pseudo C2 symmetry axis of the imidazolium ring.

Background. The most extensive work on ionic liquid structure near the metal electrode surface is from results in molten salt systems;[21] specifically, those of liquid mercury, magnesium,[22] and liquid lead electrodes in contact with metal halide salts.[23,24] Experimentally, the interfacial structure is inferred from electrocapillary and capacitance measurements. The results must be interpreted in terms of a model (an equivalent circuit) that can be quite complicated.[22] The ions in a molten salt near an electrode surface generally exhibit a layered (alternating ion) structure. Surprisingly, the potential of zero charge (PZC) of the metal/molten salt system is similar to the corresponding ions in an aqueous solution.[23] To our knowledge, there are as yet no detailed electrochemical impedance spectra (EIS) on room-temperature ionic liquids based on imidazolium cations from which the interfacial structure is deduced.

A molecular-level description on the arrangement of ions at the metal/ionic liquid interface is needed. The problem arises of how to envision double-layer structure and the potential of zero charge (PZC) in a pure liquid electrolyte. By far, most experimental and theoretical work on the double layer structure is from aqueous systems using models such as Gouy−Chapman−Sterns.[25−27] This model assumes ions are surrounded by solvation shells (of water) and have a nonuniform concentration distribution at the electrode surface that forms the diffuse double layer. This model is barely applicable to concentrated aqueous

10.1021/jp048260g CCC: $27.50
Published on Web 09/04/2004

electrolytic solutions, and is not valid in the ionic liquids where there is no solvent. Further, the results from the molten salts (as stated above) are likely to be only an approximation to the room-temperature ionic liquids discussed in this paper, since these are molecular ions and their chemical structure probably is important to the bonding and orientation at the surface. The first assumption is that ions are directly adsorbed to the surface, as in a Helmholtz layer. Also, several layers of ions may extend into the liquid to compensate for the excess surface charge. This model makes intuitive sense since the ions in the ionic liquid are relatively ordered due to high Coulombic forces. According to the Gouy−Chapmann−Stern model, the PZC is considered to be the state where the surface concentration of ions is the same as the bulk concentration.[21,27,28] However, in a pure ionic liquid with no solvent the ion concentration is essentially the same throughout the system; only in the inner Helmholtz layer is there a possible difference. There are theoretical treatments of capacitance data that show it is possible to have surface excess of ions at an electrode interface in a molten salt.[27]

Bulk Ionic Liquid Structure. Measurements on the bulk structure of an ionic liquid are useful to understand the ion interactions at the electrode surface. From the crystallographic data of 1-alkyl-3-methyl imidazolium salts containing hexafluorophosphate[29] and tetrafluoroborate,[30] it is known that the anion is centered on the cation ring. The peak shift of the aromatic hydrogen in NMR and IR spectroscopy has been used to study the interaction of ions in the ionic liquid. The results indicate that there is a slight preference for the anion toward the C(2)−H bond, however, the anion interacts with the other ring protons and thus is mostly centered on the imidazolium ring.[31−34] Computer modeling of the bulk of the ionic liquid also indicate this relative positioning of the ions.[35,36] The ion attraction is dominated by an electrostatic interaction but is also influenced by hydrogen bonding and van der Waals forces, which are determined by the anion identity. For PF_6^- and BF_4^-, these interactions are similar though the IR and NMR results indicate that the BF_4^- interaction is slightly stronger than for PF_6^-. This difference is enough to dramatically affect the physical properties such as viscosity, water miscibility, and melting point.[3,9,12,37]

To probe the molecular-level information of the ions at the electrode/ionic liquid interface, a surface-specific spectroscopic technique is used. SFG is a second order nonlinear spectroscopy technique sensitive to molecules in a noncentrosymmetric environment. Most molecules in the liquid state are considered to be in an isotropic environment; as a consequence SFG will not be generated in the bulk, but only from the liquid/electrode interface where the centrosymmetry is broken. The theory of SFG will not be covered in detail; instead, the reader is referred to different reviews.[38−44] The intensity of the SFG signal is proportional to the square of the induced polarization:

$$E_{SF} \propto P^{(2)} = |\chi^{(2)}{:}E_{vis}E_{IR}| \tag{1}$$

$$\chi^{(2)} = \chi^{(2)}_{res} + \chi^{(2)}_{nr} \tag{2}$$

$$\chi^{(2)}_{res} = \sum \frac{N\langle\beta^{(2)}\rangle}{(\omega_{IR} - \omega_q + i\Gamma_q)} \tag{3}$$

where E refers to the electric field of the visible and infrared incoming beams and $\chi^{(2)}$ is the second-order susceptibility tensor that relates the interface response to the input light fields. The $\chi_{nr}^{(2)}$ arises from the nonresonant background of the surface and the $\chi_{res}^{(2)}$ contains the molecular hyperpolarizability, $\beta^{(2)}$, with the Raman polarizability and the IR dipole transition, which are averaged over the molecule orientation indicated by the brackets, $\langle\rangle$. N indicates the number of molecules contributing to the SFG signal, ω_{IR} and ω_q refer to the frequency of the incoming IR and the normal mode, respectively, and Γ_q is the damping constant for the q^{th} vibrational mode.

Experimental Section

Sample Synthesis and Preparation. The synthesis and characterization of 1-butyl-3-methylimidazolium tetrafluoroborate, [BMIM][BF_4], and 1-butyl-3-methylimidazolium hexafluorophosphate, [BMIM][PF_6], is similar to that published by Grätzel et al.[12] 1-methylimidazole is mixed with 1-chlorobutane in a 1:1.1 molar ratio and refluxed under nitrogen at 65 °C for 52 h. The 1-butyl-3-methylimidazolium chloride, [BMIM][Cl], is washed three times with ethyl acetate and dried under vacuum at a temperature of ∼70 °C. [BMIM][Cl] is then mixed with the acid of the desired anion in a 1:1.1 molar ratio and stirred for 24 h. The final [BMIM][PF_6] compound is simply washed with water until no chloride is detected in the water. However, for the [BMIM][BF_4], it is first cooled in an ice bath and an equal volume of cold dichloromethane is added. Then, the compound is washed with ice-cold water until no chloride is detected in the water.

After [BMIM][PF_6] and [BMIM][BF_4] are dried under vacuum at a temperature of ∼70 °C, the chloride concentration is detected directly in the ionic liquid using an ion-selective electrode; both compounds have a chloride concentration ≤ 18 ppm.

All chemicals are from Aldrich and used without further purification. The water is deionized in a Millipore A10 system with a resistivity of >18 MΩ·cm and an organic concentration of < 3 ppb. H NMR, LC−MS, and FT−IR are used for characterization, and an ion selective electrode is used for the chloride determination. Cyclic voltammetry is used to estimate the water concentration (Figure 2).

The working electrode is made of polycrystalline platinum 10 mm in thickness by 0.25 in. in diameter and is prepared by flame annealing in a hydrogen−air flame for ∼10 min. The electrode is cooled in a glass chamber flowing with argon gas for 10 min. Immediately upon removal from the cooling chamber, a drop of ionic liquid is placed on the surface of the Pt electrode. The electrode is then introduced into the SFG electrochemistry cell. The procedure is analogous to the preparation of well-characterized electrodes used in aqueous electrochemistry by Clavilier,[45] where it produces a clean surface as determined by CV and UHV techniques.

The SFG-electrochemistry cell is an important development to accomplishing these experiments. The cell is vacuum-tight to $>2 \times 10^{-5}$ torr, which is possible because the Pt working electrode is held in the cell with a 1/4-in Teflon Swage fitting attached to the Kel-F shaft, (Figure 3). The entire cell is fabricated only of inert polymers (Kalrez O-rings, Teflon, or Kel-F parts) and glass, permitting aggressive cleaning in 50/50 nitric acid/sulfuric acid mixtures. The cell is thoroughly rinsed in water from a Millipore A10 water system. The counter electrode is a Pt wire and the reference is Ag/$AgBF_4$ or Ag/$AgPF_6$ that has a potential of ∼ −200 mV vs NHE (Normal Hydrogen Electrode).

Once the electrode with the ionic liquid drop on it is introduced into the cell, the cell is evacuated to its base pressure for ∼4 h at 60−70 °C. Next, a vessel containing the ionic liquid is pressurized to just over 1 atm with Ar gas. A stopcock connecting the vessel to the SFG cell is opened transferring

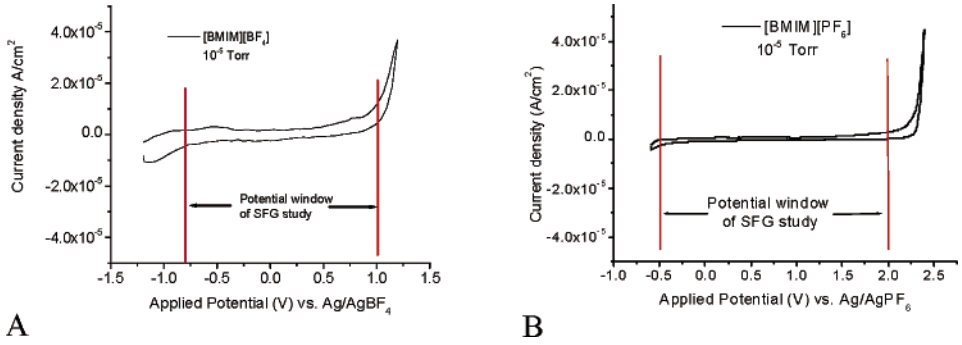

Figure 2. Cyclic voltammetry of neat (A) [BMIM][BF_4] and (B) [BMIM][PF_6] on Pt electrode. Scan rate = 100 mV/sec. Vertical red lines indicate the potential limit of the SFG experiment.

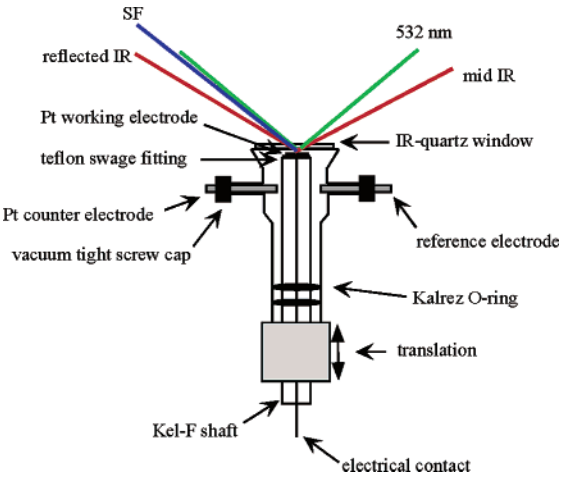

Figure 3. Thin-layer electrochemical cell for SFG studies. The reflected IR is sent to the reference channel for normalization of the SFG signal.

the ionic liquid into the SFG cell without contact to air. The cell can maintain the ionic liquid in an anhydrous state for approximately 10 h, as determined by cyclic voltammetry. The cell allows for control of potential during the SFG experiment as well as for the measurement of the CV.

Optical Setup. An Ekspla 20 Hz picosecond Nd:YAG laser is used to pump the optical parametric generation/amplification system, OPG/OPA (LaserVision). The OPG/OPA is composed of a set of KTP/KTA crystals that are used to generate the second harmonic (532 nm) and the tunable infrared beams (2000−4000 cm^{-1}). The visible beam is at an angle from the surface normal of 33° and the infrared was at an angle of 38° at the ionic liquid/Pt interface with energy densities of 30 mJ/cm^2 and 20 mJ/cm^2, respectively. Polarization control of the visible beams is accomplished by a $\lambda/2$ waveplate antireflection coated for 532 nm (CVI). The tunable infrared polarization was changed using a zero-order phase retardation plate ($\lambda/2$) supplied by ALPHALAS GmbH. Glan-Laser polarizers (CVI) are used for polarization selection in these experiments.

Optical access to the electrode surface is possible in the thin-layer cell design. The laser beams pass through an infrared quartz window, through a thin layer of ionic liquid (~10 μm thick), then travel to the Pt electrode. The generated SF signal is reflected out of the cell to the detection system described below. To verify that the SF signal is from the Pt/ionic liquid interface and not from the infrared quartz/ionic liquid interface, two tests are performed. First, the Pt electrode is backed away from the window, by ~0.5 mm, so the infrared is completely adsorbed by the ionic liquid. Under these conditions there is no SFG detected using *ssp* or *ppp* polarizations. Second, the SFG signal exhibits a potential dependence, which only occurs at the Pt/ionic liquid interface.

TABLE 1: [BMIM]BF_4]. Amplitude Values for Peaks in the SFG Spectrum of 1-butyl-3-methylimidazolium Cation on a Pt Electrode at −800 mV and +1000 mV vs Ag/$AgBF_4$ Reference. Number in Parentheses is the Percent Error of the Amplitude

	−800 mV		+1000 mV	
	ppp	ssp	ppp	ssp
CH_2(sym)	2.2 (177)	−	3.8 (15)	−
CH_3(sym)	1.0 (286)	0.9 (35)	1.6 (31)	5.1 (8)
CH_2(asym)	−	3.7 (12)	−	3.7 (36)
CH_3(asym)	−	5.7 (15)	−	4.2 (36)
CH_3(sym)(N3)	0.9 (7)	−	7.8 (3)	−
C(2)−H	1.3 (42)	1.3 (75)	3.8 (12)	−
H−C(4)C(5)−H	11 (5)	2.8 (30)	8.6 (8)	3.7 (10)
NR	−1.1	−0.07	−1.2	−0.25

Another important feature of this optical setup is the reference channel in the SFG spectrometer. The SFG signal is proportional to the infrared intensity and since the infrared intensity is not constant as a function of wavelength (due to the OPG/OPA source and absorbance in the beam path) the SFG spectra must be corrected for this. To ensure that the features in the SFG spectrum are resonances of the surface molecules and not modulations in the infrared intensity due to absorbance in the ionic liquid, the following reference procedure is used. Infrared light that is reflected from the Pt electrode is mixed in a z-cut quartz with 532-nm light and produces a reference SF signal that is only affected by the infrared fluctuations. The SFG signal is adjusted by this reference signal to compensate for the changes in infrared intensity. Since the detection system for this reference setup is identical to the one for the SFG signal, it is highly sensitive. In practice, it has been experimentally determined that the spectra can be compensated by this method if the infrared absorbance/fluctuations are less than 45%. In typical experiments, the infrared intensity change (due to absorbance) is not more than 7−8%. A reference is collected simultaneously with each SFG spectrum.

Data Collection and Analysis. The data are acquired while the infrared energy is continuously scanned from 2750 to 3300 cm^{-1} at 1 cm^{-1}/sec. Each data point in a spectrum is an average of 20 shots. The spectra presented are an average of five spectra with error bars representing the standard deviation between the spectra. The spectra are curve fitted according to eqs 1−3 using nonlinear fitting functions in Origin with instrumental setting for the error bars. As a result, the error in the peak amplitude (Table 1 and Table 2) is not only the error in the fit; it also accounts for the scatter in the data. The baselines in the spectra are at zero and are determined by blocking the infrared to collect

TABLE 2: [BMIM][PF_6]. Amplitude Values for Peaks in the SFG Spectrum of 1-butyl-3-methylimidazolium Cation on a Pt Electrode at −500 mV and +1000 mV vs Ag/$AgPF_6$ Reference. Number in Parentheses is the Percent Error of the Amplitude

	−500 mV		+1000 mV	
	ppp	ssp	ppp	ssp
CH_3(sym)	3.1 (32)	5.5 (7)	2.5 (31)	0.3 (33)
CH_2 (asym)	0.004 (5000)	−	2.0 (70)	−
N(3)CH_3(sym)	3.5 (45)	3.8 (9)	1.9 (75)	1.6 (11)
CH_3(asym)	0.018 (722)	1.3 (18)	−0.86 (100)	0.29 (48)
C(2)-H	15 (13)	−	27 (10)	−
H-C(4)C(5)-H	13 (10)	2.8 (9)	23 (3)	6.2 (4)
NR	−2.1	−0.71	−1.5	−0.44

a background signal level. The detection system contains a photomultiplier tube (Hamamatsu R3788) attached to a Jarrell-Ash monochromator. Detection electronics consist of an SRS 250 boxcar average and an SR245 computer interface board. These components are duplicated for the reference channel. The tuning of the infrared OPG/OPA (LaserVision), the monochromator, and the acquisition of SFG and reference signals are achieved by a LabVIEW program.

Results

The SFG spectra of [BMIM][BF_4] and [BMIM][PF_6] for *ppp* and *ssp* polarization are shown below in Figures 4, 5, and 6. Qualitatively, the spectra are relatively complicated. There are several resonances observed, as well as an intense nonresonant background. Therefore, only the major peaks in the spectrum are assigned and used in the analysis. The results exhibit several vibrations in the C−H stretching region that are polarization and potential dependent for both ionic liquids.

For [BMIM][BF_4] in the *ppp* spectrum, there are six resonances observed at +1000 mV. The three from the imidazolium ring are at ∼3050 cm^{-1}, 3150 cm^{-1}, and ∼3190 cm^{-1}. They are due to the interaction peak, the C(2)−H or H−C(4)C(5)−H(asym) peak, and the H−C(4)C(5)−H(sym), respectively.[32,46,47] Two other peaks at 2845 and 2870 cm^{-1} are assigned to the CH_2(sym) and the CH_3(sym) of the butyl chain.[48−50] The CH_3(sym) of the methyl group at N(3) is at ∼2935 cm^{-1}.[46,47] The peak at 3050 cm^{-1} is called the interaction peak. It is due to hydrogen-bonding interaction of the aromatic C−H bonds with the anion[32] or possibly the electrode.

In the *ssp* spectrum, there are four peaks observed. At 2875 cm^{-1} and ∼2955 cm^{-1} are the CH_3(sym) and CH_3(asym) of the butyl chain. The peaks at 2920 and 3195 cm^{-1} are from the CH_2(asym) and the H−C(4)C(5)−H(sym), respectively.

The peak intensities show a potential dependence over the range from −800 mV to +1000 mV. The CH_3(sym) disappears at low potential and reappears at high potential; the H−C(4)C(5)−H(sym) has the same behavior. In the *ppp* spectrum, peaks change intensity in a similar way.

For [BMIM][PF_6] in the *ppp* spectrum (Figure 6), six resonances are observed. Peaks at 2870 cm^{-1} and ∼2935 cm^{-1} are assigned to the CH_3(sym) of the butyl chain[48−50] and the N(3)CH_3(sym), while the peak for the CH_2(asym) is at ∼2910 cm^{-1}. The peak position, as well as the intensity, for the imidazolium ring showed a potential dependence. For the H−C(4)C(5)−H(sym), the peak shifted from 3200 cm^{-1} to ∼3170 cm^{-1} when the potential changed from +1000 mV to −500 mV. The C(2)−H vibration is clearly observed at 3130 cm^{-1} for an applied potential of −500 mV but seems to drastically decrease its intensity and shifts to ∼3100 cm^{-1} when the potential changes to +1000 mV. The interaction peak is also present in the spectra around 3030 cm^{-1}.

The *ssp* spectrum has four peaks. At 2870 cm^{-1} is the CH_3-(sym), while the peaks at 2915 and 3190 cm^{-1} are from the CH_2(asym) and the H−C(4)C(5)−H(sym), respectively (Figure

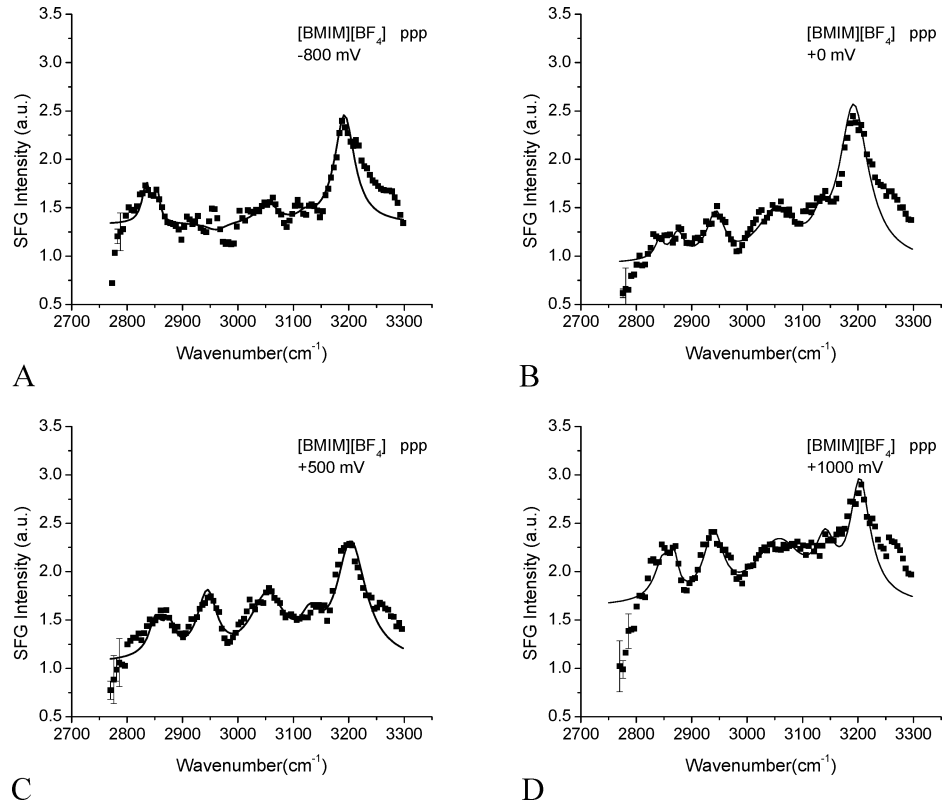

Figure 4. SFG spectra of [BMIM][BF_4] at the Pt electrode at different applied potentials. (A) −800 mV. (B) 0 mV. (C) +500 mV. (D) +1000 mV. Reference potential is Ag/$AgBF_4$. Polarization is *ppp*. Line is a fit to the line shape equation.

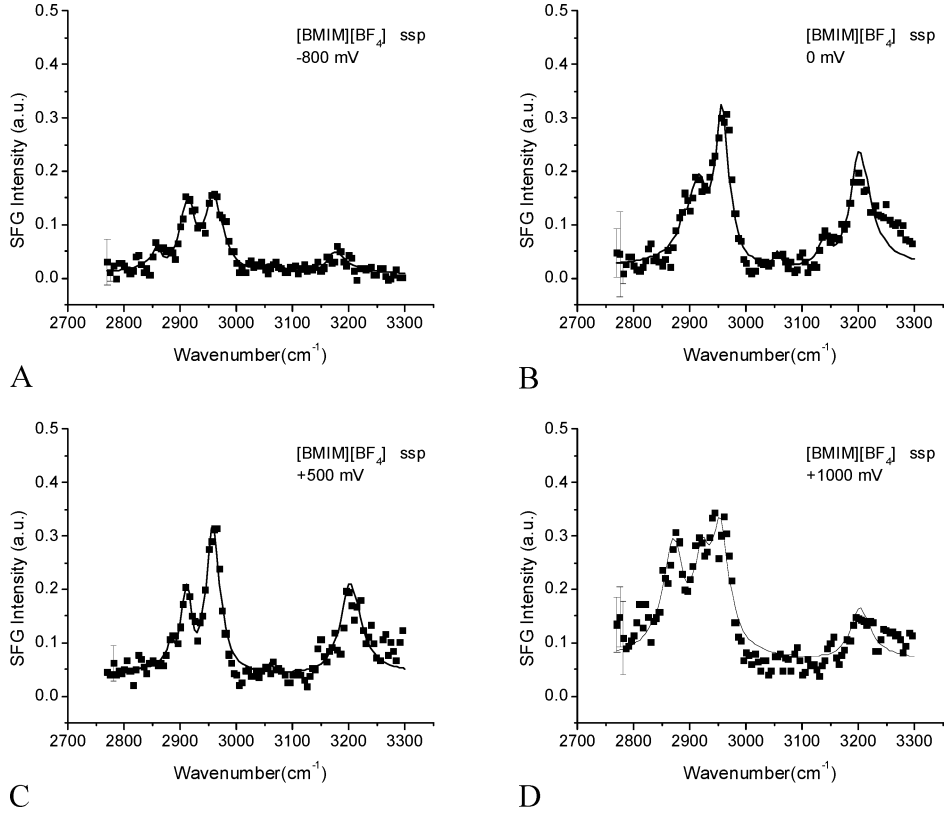

Figure 5. SFG spectra of [BMIM][BF_4] at the Pt electrode at different applied potentials. (A) −800 mV. (B) 0 mV. (C) +500 mV. (D) +1000 mV. Reference potential is Ag/$AgBF_4$. Polarization is *ssp*. Line is a fit to the line shape equation.

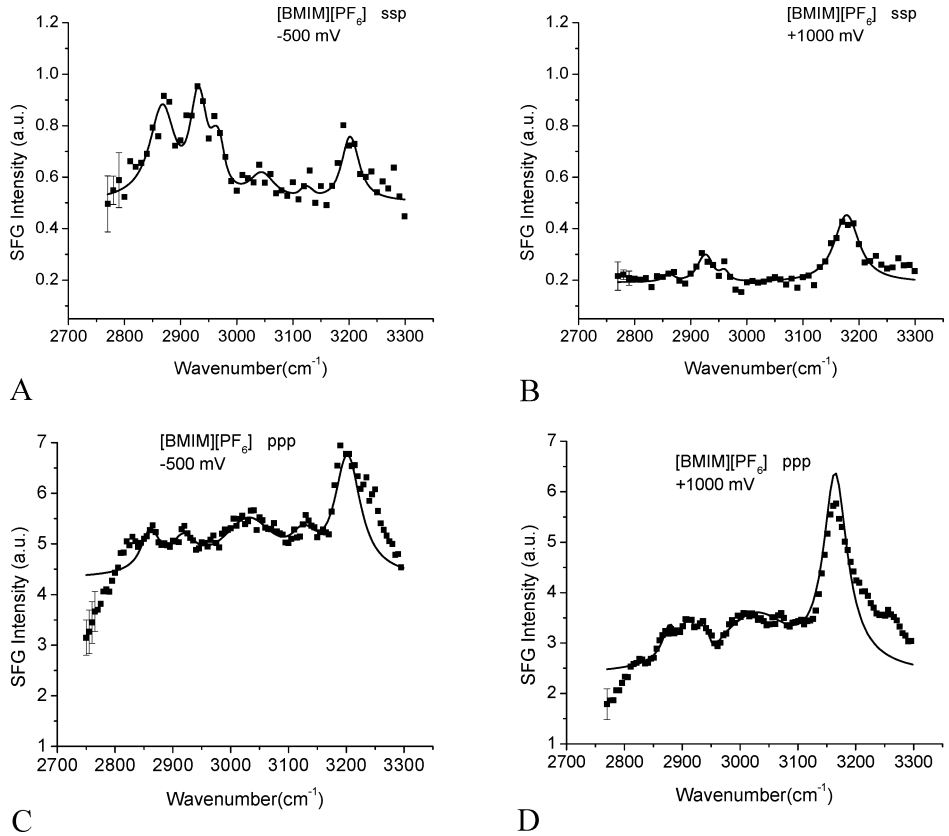

Figure 6. SFG spectra of [BMIM][PF_6] at the Pt electrode at different applied potentials. (A) −500 mV. (B) 1000 mV. A and B are for *ssp* polarization. (C) −500 mV. (D) +1000 mV. C and D are for *ppp* polarization. Reference potential is Ag/$AgPF_6$. Line is a fit to the line shape equation.

6). The resonance at 2965 cm^{-1} is due to the CH_3(asym) on the butyl chain.[48−50]

The cyclic voltammetry of ionic liquids [BMIM][BF_4] and [BMIM][PF_6] are shown in Figure 2. These are similar to the

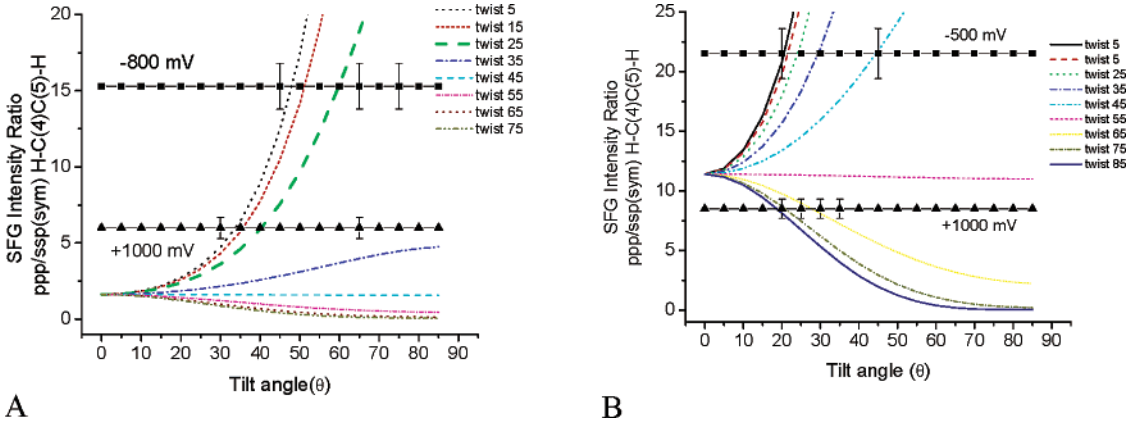

Figure 7. Simulation of SFG signal intensity ratio *ppp/ssp* for the H−C(4)C(5)−H symmetric stretch for (A) [BMIM][BF_4], (B) [BMIM][PF_6]. The filled squares (■) and triangles (▲) denote the experimentally determined ratio.

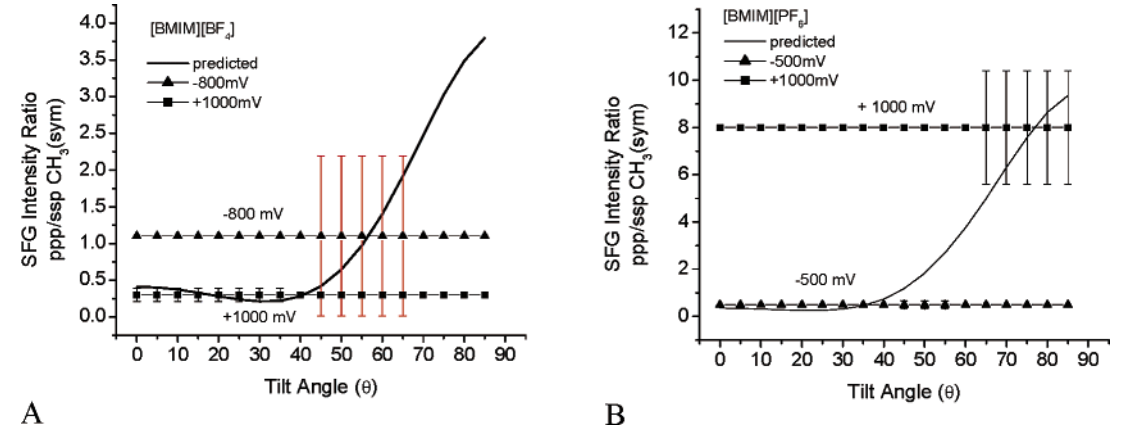

Figure 8. Orientation analysis of the terminal CH_3 group on the butyl chain of [BMIM]+. (A) [BMIM][BF_4] b) [BMIM][PF_6]. Solid line is the theoretical curve. Data points (■, ▲) are experimentally determined ratio. Note: error bars for −800 mV in A extend from 0 to +2.0.

CV reported by Xiao and Johnson.[8] and Conboy et al.[51] The potential is kept well below the oxidation and reduction limits of +2.9 to −2.0 V vs Ag/$AgBF_4$, respectively. Cyclic voltammetry of the ionic liquids indicate there is no redox processes at these potentials and the ionic liquids are relatively free of water and Cl^- (see Experimental section and Figure 2).

Discussion

Qualitatively, the peaks in the SFG spectra indicate that the imidazolium ring is oriented with the C_2 axis (Figure 1) along the surface normal. These results seem consistent with recent FTIR experiments.[52]

The orientation analysis is performed by the same method as that used by Hirose et al.[41−44] Simulations of peak intensity vs tilt angle (of the C_2 axis) are plotted for several twist angles for [BMIM][BF_4] in Figure 7A. Also plotted are the experimentally determined intensity ratio for the H−C(4)C(5)−H (3190 cm^{-1}) of the imidazolium ring in *ppp*/*ssp* spectra. The intersection of the experimental ratio with the calculated ratio indicates the possible tilt and twist angles. At +1000 mV, the C_2 axis is tilted ∼45° from the surface normal and increases to ∼60° at −800 mV. The twist angle is relatively restricted to near 0°; this is reasonable since the side chains, butyl and methyl, hinder the twist. Also, there does not appear to be a H−C(4)C(5)−H antisymmetric stretch so the H−C(4)C(5)−H plane orientation is mostly a function of tilt angle θ.

The same analysis for [BMIM][PF_6], however, indicates a different potential-dependent orientation. For this ionic liquid the tilt orientation is relatively constant from −500 mV to +1000 mV and is about 12−26° at −500 mV and 23−34° at +1000 mV. However, the twist angle changes dramatically from ∼0−35° at −500 mV to about 65−90° at +1000 mV (Figure 7B).

Although the most reliable orientation information of imidazolium is from the H−C(4)C(5)−H (sym) mode, some qualitative assessment is made by the other modes. Quantitative analysis of the alkyl CH vibrations is difficult due to the presence of nonresonant background, the many overlapping CH bands, and the interference between these two.

At +1000 mV the CH_3(sym) (2875 cm^{-1}) is strong but is absent at the other potentials while the CH_2(asym) (2915 cm^{-1}) and CH_3(asym) (2955 cm^{-1}) are intense at positive potential but weaker at negative potential. Overall, these observations indicate a higher degree of ordering along the surface normal at more positive potentials for the alkyl chains. Formal orientation analysis supports this interpretation as presented in (Figure 8). The methyl group for [BMIM][BF_4] indicates that the chain has a more perpendicular orientation at positive potentials. Thus, at + 1000 mV the tilt angle is < 40° from normal while at −800 mV it extends its range from 0 to 65°. Although this orientation preference is only slight, the increased intensity suggests an increase in polar orientation on the methyl group. In this analysis the methyl group is assigned C_{3v} symmetry and free rotation around the C−*C* axis.

For [BMIM][PF_6], the analysis of the methyl group suggests the butyl chain is more parallel to the surface > 60° at +1000 mV, while it is less than 40° at −500 mV. This is interpreted as more degrees of freedom for the alkyl chain as the imidazolium ring twists from parallel to perpendicular at the surface.

This interpretation assumes a delta function distribution and that the oriented cations do not form more than one monolayer, that is, a Helmholtz layer at the surface. From previous electrochemical studies using capacitance and electrocapillarity, this model is reasonable.[53]

To estimate the coverage of imidazolium on the electrode, cyclic voltammetry is used. The PZC of 1-ethyl-3-methylimidazolium-BF_4 was determined by Koch et al.,[53] and found to be -0.5 V vs Ag/AgCl ($\sim$Ag/AgBF_4). By integrating the double-layer current from PZC to a given potential in the Pt electrode, the charge accumulation is estimated. For [BMIM][BF_4], integration from -0.5 V to 1 V is approximately 2.8×10^{-4} C/cm^2, assuming an atomically flat surface (otherwise a roughness factor of 2$-$3 should be applied).[25] This charge value is in agreement with those calculated from differential capacitance. The capacitance at the Hg/[EMIM][BF_4] is on the order of 1×10^{-5} F/cm,[2,53] which is a surface charge of about 1×10^{-4} C, or 0.5 monolayer of electric charge ($\sim 2 \times 10^{-4}$ C/monolayer). Using this estimate on the amount of surface charge it seems reasonable to envision that the ions adsorb to the surface as a single layer and multilayers are not present at the surface. This is consistent with a Helmholtz model of the interface.

The SFG data suggest that at high positive potential the cation, $[BMIM]^+$, is tipped with the imidazolium ring along the surface normal and the ring becomes more parallel to the surface at more negative potentials. This is reasonable since the PZC of this system is near -500 mV;[53] thus, at -800 mV the surface has a negative charge. Previous results have shown that the cation charge is mostly centered on the aromatic ring;[54,55] thus, this would be the lowest energy situation considering only the electrostatic energy. To screen the charge, the ring orients parallel to the surface. At positive surface charge the anion will move into the inner Helmholtz layer for charge compensation and the cation will then occupy the outer Helmholtz layer. This model suggests that the cation is tipped along the surface normal to make room for the anion to approach the surface at potentials positive of PZC. Further, the effect is different for $[BF_4]^-$ compared to $[PF_6]^-$ and is likely due to its size and/or charge density.

There appears to be two slightly differing mechanisms for cation reorientation at the electrode surface. In the case of negative surface charge, the imidazolium ring is relatively parallel to the electrode surface, presumably to screen the surface charge. However, when the surface charge becomes positive the ring tips from the surface to allow space for the anion to enter the Helmholtz layer and shield the electrode charge. For the [BMIM][BF_4] and [BMIM][PF_6] ionic liquids this occurs in two different ways. In the [BMIM][BF_4] case, the twist angle of the ring is not greatly different at the positive and negative potentials and only the tilt angle changes. However, for [BMIM][PF_6] the tilt angle is not changing as a function of potential, but instead is changing with respect to the twist angle. These results suggest that $[BMIM]^+$ changes its polar tilt angle (θ) to allow the anion access to the surface for $[BF_4]^-$ while it changes its twist angle to allow $[PF_6]^-$ access to the surface.

Conclusion

Sum frequency generation has been used to study the adsorption and orientation of ions in a room-temperature ionic liquid at the platinum electrode surface. The results indicate that the cation has a preferred orientation that changes as a function of applied potential. At relatively negative surface charge the imidazolium ring is nearly parallel to the surface, while it tilts along the surface normal at more positive potential.

Acknowledgment. We gratefully appreciate funding for this project provided by The Welch Foundation (E1531) and The Petroleum Research Fund (37767.01-G5).

References and Notes

(1) Seddon, K. R. *J. Chem. Technol. Biotech.* **1997**, *68*, 351.
(2) Fuller, J.; Carlin, R. T.; Osteryoung, R. A. *J. Electrochem. Soc.* **1997**, *144*, 3881.
(3) Quinn, B. M.; Ding, Z.; Moulton, R.; Bard, A. J. *Langmuir* **2002**, *18*, 1734.
(4) Welton, T. *Chem. Rev.* **1999**, *99*, 2071.
(5) Suarez, P. A.; Einloft, S.; Dullius, J. E.; Souza, R. F.; Dupont, J. *J. Chim. Phys.* **1998**, *95*, 1626.
(6) Holbrey, J. D.; Seddon, K. R. *Clean Products and Processes* **1999**, *1*, 223.
(7) Trulove, P. C.; Mantz, R. A. Electrochemical Properties of Ionic Liquids. In *Ionic Liquids in Synthesis*; Welton, T., Wasserscheld, P., Eds.; Wiley-VCH: Morlenbach, 2003; p 368.
(8) Xiao, L.; Johnson, K. E. *J. Electrochem. Soc.* **2003**, *150*, E307.
(9) Suarez, P. A.; Selbach, V. M.; Dullius, J. E.; Einloft, S.; Pianicki, C. M.; Azambuja, D. S.; deSouza, R. F.; Dupont, J. *Electrochim. Acta* **1997**, *42*, 2533.
(10) Doyle, M.; Choi, S. K.; Proulx, G. *J. Electrochem. Soc.* **2000**, *147*, 34.
(11) Hagiwara, R.; Hirashige, T.; Tsuda, T.; Ito, Y. *J. Electrochem. Soc.* **2002**, *149*, D1.
(12) Bonhote, P.; Dias, A.; Papageorgiou, N.; Kalyanasundaram, K.; Grätzel, M. *Inorg. Chem.* **1996**, *35*, 1168.
(13) Papageorgiou, N.; Anthanassov, Y.; Armand, M.; Bonhte, P.; Pettersson, H.; Azam, A.; Gratzel, M. *J. Electrochem. Soc.* **1996**, *143*, 3009.
(14) Rogers, R. D.; Huddleston, J. G.; Williauer, H. D.; Swatloski, R. P.; Visser, A. E. *Chem. Commun.* **1998**, 1765.
(15) Abraham, M. H.; Zissimos, A. M.; Huddleson, J. G.; Willauer, H. D.; Rogers, R. D.; Acree, W. E. *Ind. Eng. Chem. Res.* **2003**, *42*, 413.
(16) Dupont, J.; deSouza, R. F.; Suarez, P. A. *Chem. Rev.* **2002**.
(17) Suarez, P. A.; Dullius, J. E.; Einloft, S.; DeSouza, R. F.; Dupont, J. *Polyhedron* **1996**, *15*, 1217.
(18) Wilkes, J. S.; Levisky, J. A.; Wilson, R. A.; Hussey, C. L. *Inorg. Chem.* **1982**, *21*, 1263.
(19) Wilkes, J. S.; Zaworotko, M. J. *J. Chem. Soc., Chem. Commun.* **1992**, 965.
(20) *Ionic Liquids in Synthesis*; Welton, T.; Wasserscheid, P., Eds.; Wiley-VCH: Morlenbach, 2003, p 364.
(21) Bockris, J. O.; Khan, S. U. M. *Surface Electrochemistry*, 1st ed.; Plenum Press: New York, 1993.
(22) Kisza, A. *J. Electroanal. Chem.* **2002**, *534*, 99.
(23) Graves, A. D. *Electroanal. Chem.* **1970**, *25*, 349.
(24) Graves, A. D.; Inman, D. *Electroanal. Chem.* **1970**, *25*, 357.
(25) Bard, A. J.; Faulkner, L. R. *Electrochemical Methods*, 2nd ed.; John Wiley and Sons: New York, 2001.
(26) Schmickler, W. *Interfacial Electrochemistry*, 1st ed.; Oxford University Press: New York, 1996.
(27) Bockris, J. O.; Reddy, A. K. N. *Modern Electrochemistry: Ionics*, 2nd ed.; Plenum Press: New York, 1998; Vol. 1.
(28) Devanathan, M. A.; Tilak, B. V. *Chem. Rev.* **1965**, *65*, 635.
(29) Gordon, C. M.; Holbrey, J. D.; Kennedy, A. R.; Seddon, K. R. *J. Mater. Chem.* **1998**, *8*, 2627.
(30) Holbrey, J. D.; Seddon, K. R. *J. Chem. Soc., Dalton Trans.* **1999**, *13*, 2133.
(31) Carmicheal, A. J.; Hardacre, C.; Holbrey, J. D.; Seddon, K. R.; Nieuwenhuyzen, M. *Proc. Electrochem. Soc.* **2000**, *99*$-$*41*, 209.
(32) Dieter, K. M.; Dymek, C. J.; Heimer, N. E.; Rovang, J. W.; Wilkes, J. S. *J. Am. Chem. Soc.* **1988**, *110*, 2722.
(33) Fannin, A. A.; King, L. A.; Levisky, J. A.; Wilkes, J. S. *J. Phys. Chem.* **1984**, *88*, 2609.
(34) Haung, J. F.; Chen, P. Y.; Sun, I. W.; Wang, S. P. *Inorg. Chim. Acta* **2001**, *320*, 7.
(35) Urahata, S. M.; Ribeiro, M. C. *J. Chem. Phys.* **2004**, *120*, 1855.
(36) Morrow, T. I.; Maginn, E. J. *J. Phys. Chem. B.* **2002**, *106*, 12807.
(37) Cammarata, L.; Kazarian, S. G.; Salter, P. A.; Welton, T. *Phys. Chem. Chem. Phys.* **2001**, *3*, 5192.
(38) Shultz, M. J.; Baldelli, S.; Schnitzer, C.; Simonelli, D. *J. Phys. Chem. B* **2002**, *106*, 5313.
(39) Buck, M.; Himmelhaus, M. *J. Vac. Sci. Technol., A* **2001**, *19*, 2717.
(40) Huang, J. Y.; Shen, Y. R. Sum Frequency Generation as a Surface Probe. In *Laser Spectroscopy and Photochemistry on Metal Surfaces*; Dai, H. L., Ho, W., Eds.; World Scientific: Singapore, 1995.
(41) Hirose, C.; Yamamoto, H.; Akamatsu, N.; Domen, K. *J. Phys. Chem.* **1993**, *97*, 10064.
(42) Hirose, C.; Akamatsu, N.; Domen, K. *Appl. Spectrosc.* **1992**, *46*, 1051.

(43) Hirose, C.; Akamatsu, N.; Domen, K. *J. Chem. Phys.* **1992**, *96*, 997.
(44) Akamatsu, N.; Domen, K.; Hirose, C. *J. Phys. Chem.* **1993**, *97*, 10070.
(45) Clavilier, J.; Faure, R.; Guinet, G.; Durand, R. *J. Electroanal. Chem.* **1980**, *107*, 205.
(46) Carter, D. A.; Pemberton, J. E. *J. Raman Spectrosc.* **1997**, *28*, 939.
(47) Carter, D. A.; Pemberton, J. E.; Woelfel, K. J. *J. Phys. Chem. B* **1998**, *102*, 9870.
(48) MacPhail, R. A.; Strauss, H. L.; Snyder, R. G.; Elliger, C. A. *J. Phys. Chem.* **1984**, *88*, 334.
(49) Snyder, R. G. *J. Chem. Phys.* **1965**, *42*, 1744.
(50) Snyder, R. G.; Strauss, H. L.; Elliger, C. A. *J. Phys. Chem.* **1982**, *86*, 5145.
(51) Fitchett, B. D.; Knepp, T. N.; Conboy, J. C. *J. Electrochem. Soc.* **2004**, *in press*.
(52) Nanbu, N.; Sasaki, Y.; Kitamura, F. *Electrochem. Commun.* **2003**, *5*, 383.
(53) Nanjundiah, C.; McDevitt, S. F.; Koch, V. R. *J. Electrochem. Soc.* **1997**, *144*, 3392.
(54) Hardacre, C.; Holbrey, J. D.; McMath, S. E.; Bowron, D. T.; Soper, A. K. *J. Chem. Phys.* **2003**, *118*, 273.
(55) Hanke, C. G.; Price, S. L.; Lyndon-Bell, R. M. *Mol. Phys.* **2001**, *99*, 801.